

H14-287

PROPER ORTHOGONAL DECOMPOSITION OF VERY TURBULENT FLOW INSIDE AN URBAN STREET

Radka Kellnerova^{1,2}, Libor Kukacka^{1,2}, Vaclav Uruba¹, Klara Jurcakova¹ and Zbynek Janour¹¹Institute of Thermomechanics AS CR, v.v.i, Department of Fluid Dynamics, Czech Republic²Department of Meteorology and Environment Protection, Charles University, Czech Republic

Abstract: Wind-channel experiment of simulation of turbulent boundary layer above urban street canyons was performed. Two geometries of canyons are tested – building with flat and triangle roof. Attention is paid to the main dynamical phenomena that have direct impact on a flow regime in the canyon. The POD is applied on velocity data. Fourier analysis and Wavelet analysis is then used to reveal the frequency and temporal information of the significant events in the flow. Sensitivity of this method is tested in relation to the sample frequency of measurement technique PIV.

Key words: street canyon, POD, Fourier spectrum, Wavelet spectrum.

INTRODUCTION

This contribution describes the character of turbulent flow generated above series of street canyons in wind-channel. Main concern is to clarify how intermittent dynamics of the flow determines the ventilation process inside the canyon. In this first part of study, only the flow character is investigated. Since geometry of building around street canyon significantly affects the flow regime, two shapes of building (triangle and flat) are studied and comparison of these two regimes is done by POD method. Further, a sensitivity of POD on input data is investigated. Especially, the test concerning the sample frequency of PIV techniques is performed in order to evaluate a minimum spatial resolution for POD.

EXPERIMENTAL SET-UP

The roughness on the floor of the channel represents long series of identical and parallel street canyons (Figure 1). Aspect ratio between the width and the height of street equals to one. Channel itself has a dimension of 0.25 m x 0.25 m in cross-section and about 3 m in longitudinal direction. Since the street is 0.05 m high, the dimension of canyon is rather large with respect to the dimension of the channel. This can cause an aerodynamic blockage what can generate an undesired dynamics in the turbulent flow. From this reason, the flow above the street canyons in wind-channel was carefully measured and quantitatively compared with regular boundary layer in a wind-tunnel. Time-mean velocity, momentum fluxes and spectral density analysis showed that the region within the street canyon can be considered as representative one. However, the region above the roof-top level deviates from right values. The higher is elevation, the bigger discrepancy occurs. Thus, we restricted the area of PIV measurement up to the level $Z/H=1.5$, where Z is vertical coordinates and H is height of the street canyon. In longitudinal direction, the area of interest lies as far as possible (2 m) from the mouth of the channel in order to fulfil requirements for development of well-balanced turbulent boundary layer (Cheng & Castro, 2002). Reference velocity at the mouth of the channel is 5 m/s.

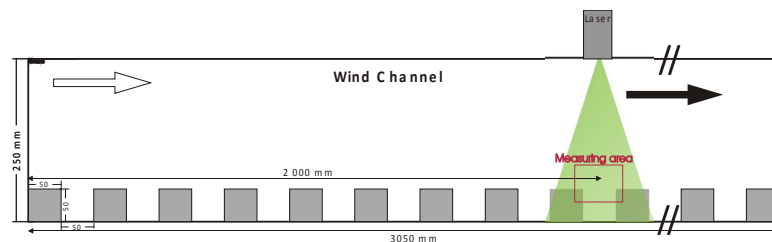


Figure 1: Scheme of the channel and laser sheet. Investigated XZ plane is in the middle of channel.

Time-resolved PIV (500 Hz) is used to record 2-D velocity vectors in vertical plane X-Z, where X-direction is horizontal axes parallel to the approaching flow and Z-direction is vertical axes. Camera has resolution of 1280 x 1024 pixels. The illuminated area is 0.1 m x 0.1 m large and involves more than 4800 vectors, since we use overlapping of 50% in post-processing. Spatial resolution of PIV results in 1.2 mm. Data were recorded over time of 3.2 s in each run. By this, we got more than 1600 snapshots in one run.

RESULTS

Velocity information (U- and W-component) in snapshots is decomposed by Proper orthogonal decomposition (POD) (Lumley, 1967, Hertwig, 2009). The most dominant modes from the TKE point of view are achieved. The most important phenomena reveal to be a formation of vortices behind the roof, an intensification of the vortex inside the street, sweep and ejection events in the main flow or formation of various vortices in various locations. All POD modes are derived from velocity fluctuations, so they represent the intermittent behaviour of system.

Every mode has its own weight factor that is a function of time. When an extreme appears in this time-evolution of weight factor, the particular mode plays a significant role for a moment. We confronted temporal position of peaks with PIV records and successfully assigned the relevant mode to their dynamical events. To show, how the modes look like, in Figure 2 are displayed the first four modes for pitched roof case. The first mode represents a vortex behind roof, second one a vortex between the walls, third one depicts dominant sweep (or ejection) event and last one is about recirculation with core near the

bottom of street. From record can be seen that even the fourth mode with only 4 % of TKE is crucial for the dynamics and entirely modifies the general flow.

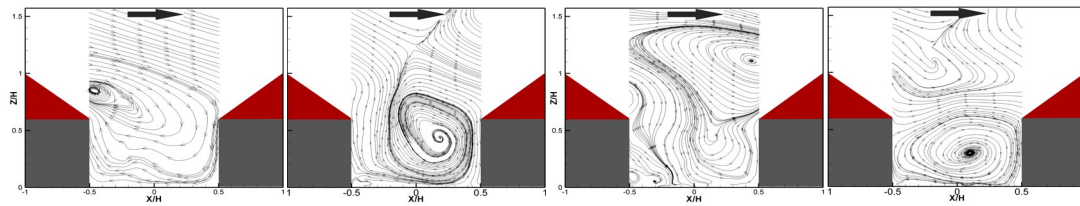


Figure 2. The four most dominant spatial modes (topos) displayed with pseudo-streamlines for pitched roof geometry: from the left: a) first mode, b) second mode, c) third mode, d) fourth mode. Black arrow on the top shows the direction of the approaching flow.

The expansion coefficients exhibit some repetitive patterns. For example, the local maximum of the first coefficient is often followed by local maximum of the second coefficient (see Figure 3). With certain level of simplification, we can draft a scenario of flow dynamics. These scenarios are visible in Figure 3 around snapshots number 200, 470 and 580, where large peaks in Mode 1 take place. Scenario could be described by following scheme: on the very beginning, fast approaching flow causes a formation of vortex behind the roof (positive Mode 1) while passing over the roof vertex. The sweep event on the upper boundary of this vortex (negative Mode 3) enters into the canyon and spins up the recirculation between walls (positive Mode 2). The recirculation is pressed downwards by new incoming air (positive Mode 4). Sometime, the low vortex (positive Mode 4) undertakes an outstanding intensification and produces a strong ejection event (positive Mode 3) afterwards.

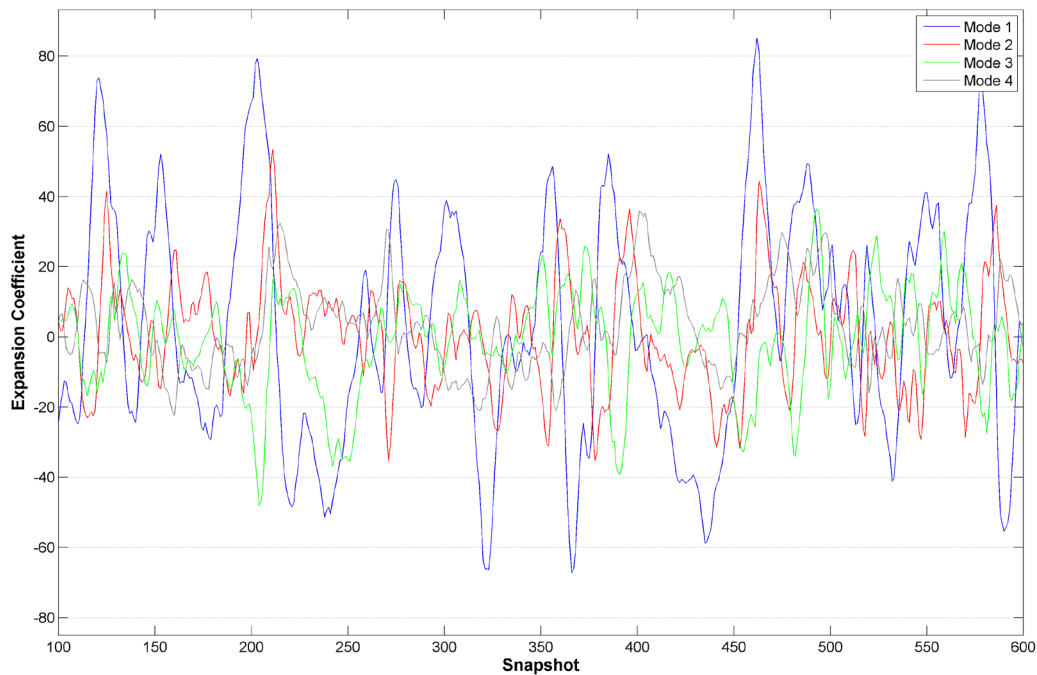


Figure 3. Example of temporal evolution of expansion coefficients for four POD modes. Each colour corresponds to one POD mode.

We derived mutual correlation amongst all expansion coefficients of the first four modes (see Figure 4). Between the first and the second mode, the correlation reaches up to 0.45 for temporal lag of 14 ms. It means that once the vortex behind roof is established, the strong downdraft on its upper boundary penetrates into canyon and speeds up the rotation between the wall after 14 ms. Likewise, there is marked negative peak at time lag of -12 ms, what suggests that the decelerated rotation of vortex between walls precedes the formation of vortex behind the roof by 12 ms.

Generally, the strongest correlation (0.48) is amid second and fourth modes, since they both represent the vortices at slightly different position. At first, the vortex between walls is formed (getting energy from penetration of the flow associated with Mode 1) and in 12 ms later, the lower vortex receives sufficient level of energy to spin up. Since, the vortex behind the roof is always accompanied by certain kind of sweep event, one would expect higher level of correlation between vortex behind roof (positive Mode 1) and sweep (negative Mode 3). Nevertheless, the linkage is very weak, reaches only correlation level of -0.1 at time lag of -8 ms. There slightly stronger connection (0.4) between roof vortex and final ejection event at time lag of 28 ms. It implies that dynamics starting with vortex behind roof and going through all the before-mentioned stages ends up by ejection event.

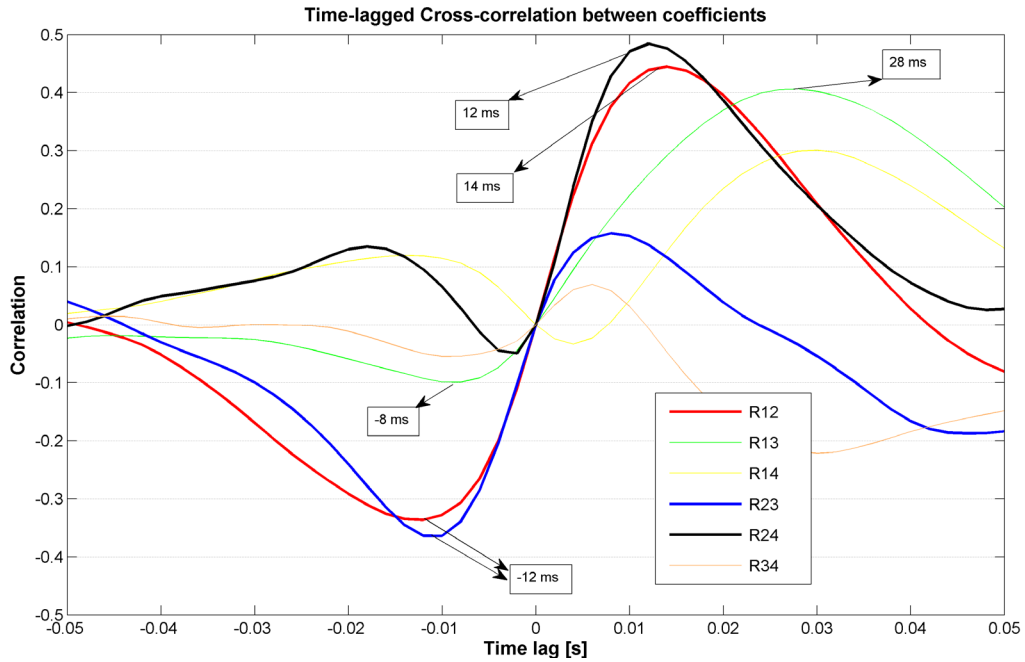


Figure 4. Time-lagged cross-correlation between particular expansion coefficients (e.g. R12=correlation between expansion coefficients of Mode 1 and Mode 2). Thick line labels the correlations with significant maximum.

By linear combination of modes we can reconstruct each of the original snapshot. The fewer modes we employ, the less accurate reconstruction we get. In Figure 5 is plotted relative error (based on Frobenius norm) against the number of modes involved in calculation for pitched case. When one considers the relative error of 10% as accurate enough, only the 6 most dominant modes can be used. However, to reach a relative error of reconstruction lower than 5%, more than 400 principal modes have to be combined. Figure 5 expresses rather gradual decrease, so the significance of the modes with higher number is non-negligible.

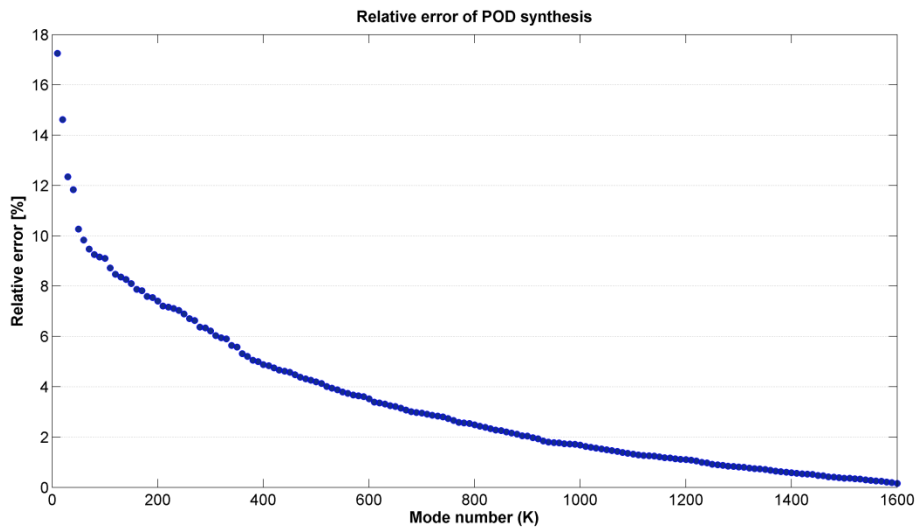


Figure 5. Relative error of synthesis for pitched case. The error is calculated for 1600 snapshots with all 1600 modes and averaged over all snapshots. Calculation is based in Frobenius norm.

We tested sensitivity of POD method on sample frequency. While reducing the sample frequency, we calculated the POD modes and their expansion coefficients. During the test, we involved in computation only every 2th snapshot, then every 4th, every 8th and every 16th, eventually. In Figure 6 is plotted convergence of relative contributions of energy from particular modes to the total turbulent kinetic energy. The first mode contains 32% of TKE. The POD keeps the same percentage of the TKE while reducing the sample frequency from all snapshots (labelled 1) to every 4th snapshot (labelled 4). Only when we involved solely every 8th or 16th mode, the result changes. Minimum spatial resolution in this case can be preliminarily evaluated as 8 ms (~125 Hz).

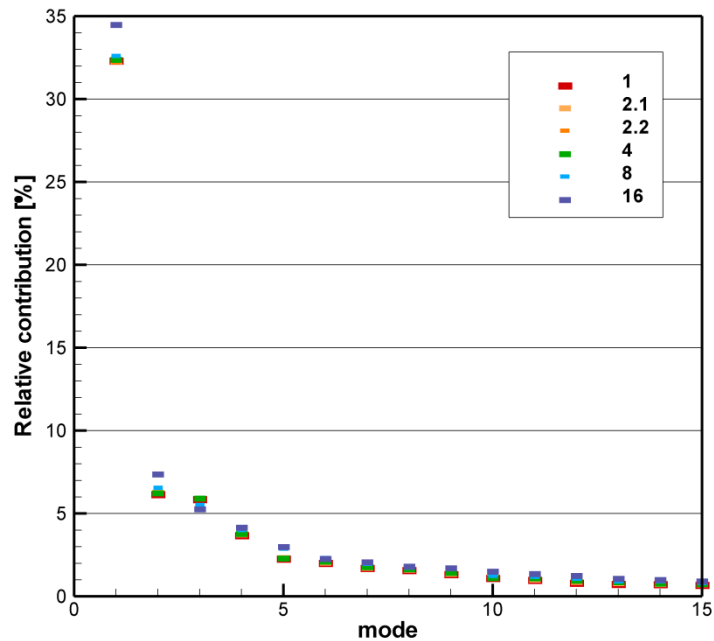


Figure 6. Relative contribution of energy to the total TKE of the system from each mode. When using all snapshots (every one), result is marked as 1. When using every second snapshot, results are marked as 2.1 and 2.2, depending if we took the 1st, 3rd, 5th snapshot and so on or if we took the 2nd, 4th, 6th and so on. Results labelled as 4, 8 and 16 means that we used every 4th, 8th and 16th snapshots in test.

Time series of weight factors can be analysed by Fourier spectral as well as Wavelet analysis. For Fourier spectral analysis, results are very similar to the spectral analyses of ‘ordinary’ velocity (Figure 7). The 1D velocity (U-component) is measured by hot-wire (CTA, Gold-plated Dantec 55 P01) with sampling frequency of 25 kHz. The Fourier spectral analysis of POD coefficients is obtained from PIV measurement (2D, U- and W- component, 500Hz).

For example, Mode 1,2 and 3 show that the spectral peaks belong into same frequency range around 10 Hz as the velocity peak. Mode 4 has its peak of energy shifted more toward a lower frequency, with maximum at 5 Hz. It is necessary to mention that acquisition time of single PIV run was only 3.2 s and therefore the spectral information in very low frequency (around 1 Hz) is not representative. Unfortunately, the Fourier spectral analysis does not bring any further information about POD modes.

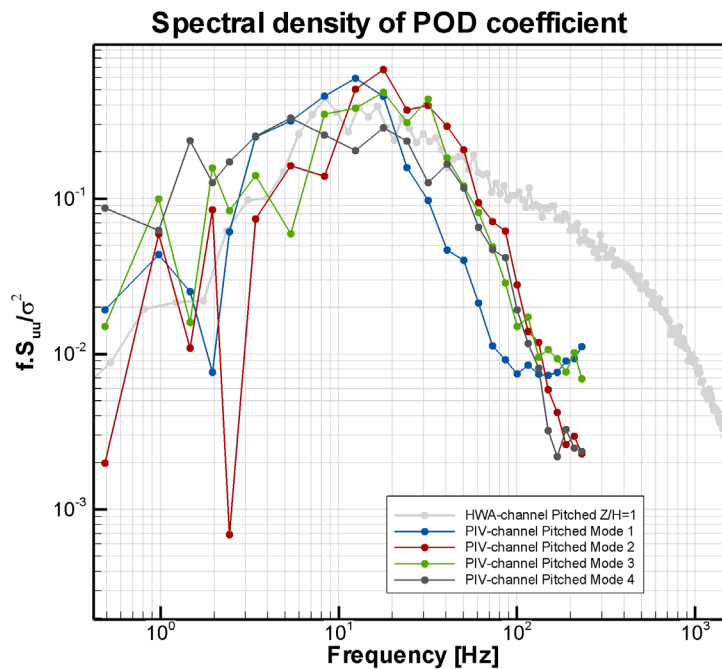


Figure 7. Fourier spectral analysis of U-component of velocity at Z/H=1 (obtained from HWA) - light grey line. The spectral analysis of POD expansion coefficients (obtained from PIV) - other colours.

On the other hand, Wavelet analysis is capable to reveal temporal location of energetic event together with the spectral information (Addison, 2002). We used a Morlet function as a mother wavelet and adopted the algorithm from Torrence and

Compo (1998). It was found out that Wavelet spectral diagram (so-called scalogram) of POD coefficients are very similar to the ones, derived from velocity data (Kellnerova et al., 2011). We calculated scalogram in every position in street canyon for both U- and W- velocity components. Then we computed the deviation of individual Wavelet scalograms from reference scalogram of POD coefficient for the first Mode 1. By this, not only spectral density of energy came into question but also the temporal positions of energetically significant event were considered.

In Figure 8 is depicted the 3-D view on deviation between the velocity scalograms and the reference POD scalogram. The left picture shows the comparison between U-component of velocity and the first expansion coefficient (labelled a_1). The lowest values appears in the elevation of $Z/H=1.2$. The area of relatively low deviation extends over whole width of the street. It is worthy to emphasise, that Frobenius norm is rather strict, so even a minute deviation of scalogram results in big relative difference. Hence, the lowest value of deviation drops down to 27%, despite the apparent similarity of two scalograms (Kellnerova et al., 2011).

For the W-component, the situation is not the same. In Figure 8 – right we can see that the similarity level is very poor.

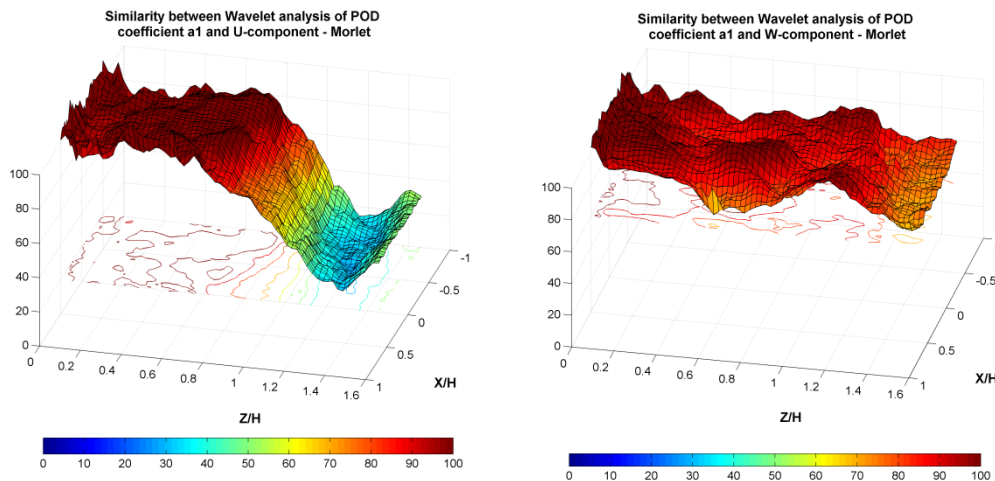


Figure 8. Similarity between wavelet scalogram of POD coefficient a_1 (whole spatial extent of the street canyon) and U-component (left) or W-component (right) at various positions.

Similarity between Wavelet of velocity and POD coefficient is not causeless. When we accept the presumption that dynamics of the system is reliably captured in Wavelet scalogram then we can conclude: the dynamics of the POD mode is driven by horizontal flow within the horizontally extended area at level around $Z/H=1.2$.

CONCLUSION

POD analysis helped to decompose such a complex turbulent flow into more simple modes. We presented character of the first four modes herein. The modes with higher number however still play important role in flow physics. From time to time, even a mode with small contribution to the turbulent kinetic energy can be predominant in the flow.

Wavelet analysis becomes a useful tool for evaluation of mutual linkage between spatial regions and POD modes in terms of dynamics. Herein just for the purpose of the paper, the dynamics is supposed to be 'fully' described by the Wavelet analysis. Then we can say that the area with dynamics similar to the dynamics of POD coefficient is governing for shape of the mode. So, we can find the area with essential impact on formation of particular POD modes.

REFERENCES

- Adisson P. S., 2002: The Illustrated Wavelet Transform Handbook. *Institute of Physics Publishing*, Bristol, 2002.
- Cheng H. and Castro I. P., 2002: Near-Wall Development After a Step Change in Surface Roughness. *Boundary Layer Meteorology*, **105**, 411- 432.
- Hertwig, D., 2009: Detection of coherent structures in atmospheric boundary layer flows: a comparative wind tunnel study using POD, LSE and wavelets. *Diploma thesis*, University of Hamburg.
- Kellnerova R., Kukacka L., Janour Z., 2011: Proper Orthogonal Decomposition of Velocity and Vorticity Field Within the Street Canyon and Wavelet Analysis of the Expansion Coefficients. *Physmod 2011- International Workshop on Physical Modeling of Flow and Dispersion Phenomena, Conference proceeding*, 90-98.
- Lumley J. L., 1967: The structure of inhomogeneous turbulent flows. In A. M. Yaglom and V. I. Tatarski, editors, *Atmospheric Turbulence and Radio Wave Propagation*, 166-178.
- Torrence C. and Compo G. P., 1998: A Practical Guide to Wavelet Analysis. *Bull. Am. Meteorol. Soc.*, **79**, 61-78.